

# The Fragmentation of Alkoxychlorocarbenes in Hydrocarbon Solvents and in Low Temperature Argon Matrixes

Robert A. Moss,\* Yan Ma, Fengmei Zheng, and Ronald R. Sauers\*

Department of Chemistry and Chemical Biology, Rutgers, The State University of New Jersey, New Brunswick, New Jersey 08903

Thomas Bally\* and Alexander Maltsev

Institute for Physical Chemistry, University of Fribourg, Perolles, CH-1700 Fribourg, Switzerland

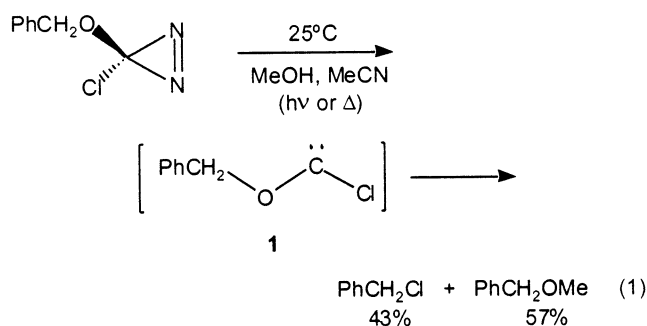
John P. Toscano and Brett M. Showalter

Department of Chemistry, Johns Hopkins University, Baltimore, Maryland 21218

Received: July 23, 2002; In Final Form: October 15, 2002

Alkoxychlorocarbenes (ROCCl, R = benzyl, cyclohexyl, and 1-octyl) were generated from the corresponding diazirines in acetonitrile, dichloroethane, benzene, cyclohexane, and pentane solutions at 25 °C, and the fragmentations of these carbenes were examined. Formation of RCl (and alkenes when R = cyclohexyl or 1-octyl) occurred efficiently in all of the solvents. The rate constant for the fragmentation of PhCH<sub>2</sub>OC(=O)Cl (determined by laser flash photolysis) was  $\sim 10^5$  s<sup>-1</sup>, and relatively independent of solvent. Photolysis of PhCH<sub>2</sub>OC(N<sub>2</sub>)Cl in Ar matrixes led to the carbene, PhCH<sub>2</sub>OC(=O)Cl, as well as its primary fragmentation products, the benzyl and COCl radicals. A prominent product was also phenacyl chloride, PhCH<sub>2</sub>COCl, a formal rearrangement product of the carbene. Computational studies of the rearrangements and fragmentations of MeOC(=O)Cl, EtOC(=O)Cl, and PhCH<sub>2</sub>OC(=O)Cl at the DFT and coupled cluster levels afforded transition states and energetics. These studies allowed us to identify several mechanistic pathways, including concerted and homolytic processes that are predicted to prevail in nonpolar solvents and matrixes as opposed to heterolytic (ionic) processes in polar solvents. The existence of cis and trans forms of R–OC(=O)–Cl, and their interconversion, are complicating factors that were considered computationally.

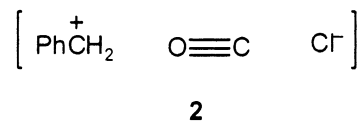
In polar solvents such as acetonitrile, methanol, or 1,2-dichloroethane (DCE), benzyloxychlorocarbene (**1**) fragmented to benzyl chloride, carbon monoxide, and solvent trapping products (e.g., benzyl methyl ether in methanol); cf., eq 1.<sup>1</sup> It



is known that *both* cis and trans forms of MeOC(=O)Cl and PhOC(=O)Cl are generated by diazirine photolysis in cryogenic matrixes,<sup>8</sup> and for purposes of interpretation and discussion it seems most reasonable to assume that this is also the case for the photolytic generation of PhCH<sub>2</sub>OC(=O)Cl in ambient temperature solution as well. (In Ar matrixes, both cis and trans isomers of **1** are formed, see below.)

Stereochemical retention during the fragmentation of chiral  $\alpha$ -deuterio-**1**,<sup>2</sup> as well as the persistence of 43% of benzyl chloride even when the reaction occurred in methanol,<sup>1</sup> led to

a mechanistic formulation of the fragmentation via ion pair **2**.<sup>1,3</sup> The absolute rate constant of the fragmentation, measured by

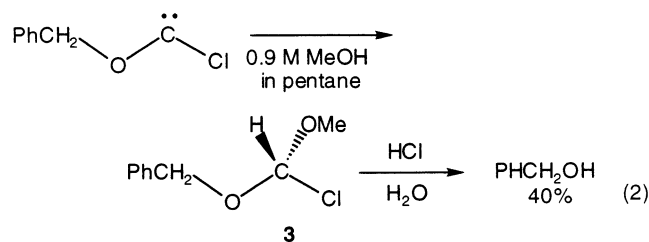


laser flash photolysis (LFP) using either UV<sup>4,5</sup> or time-resolved infrared (TRIR) monitoring,<sup>5</sup> gave  $k_{\text{frag}} \sim 4.5 \times 10^5$  s<sup>-1</sup> (MeCN) and  $\sim 1.8 \times 10^5$  s<sup>-1</sup> (DCE).<sup>5</sup>

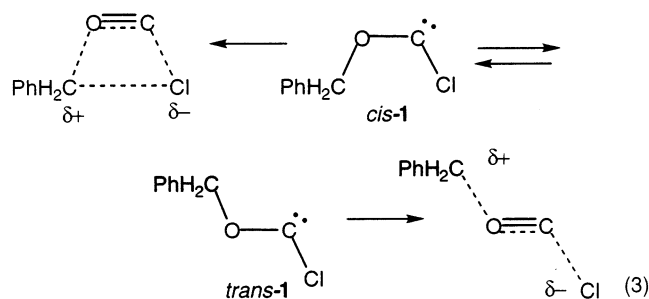
In polar solvents, ionic fragmentation is fast enough such that trapping of the carbene by MeOH is not competitive; no carbene–methanol products are observed.<sup>1,3,6</sup>

However, we would not expect ionic fragmentation in nonpolar solvents. Indeed, in 0.9 M MeOH in pentane (as opposed to MeOH in MeCN), up to 40% of **1** is trapped by the methanol affording benzyl alcohol, presumably by the sequence in eq 2, where traces of water and/or HCl hydrolyze the initially formed chloroacetal (**3**).<sup>1,7</sup> The yield of benzyl chloride is not affected on going from acetonitrile to methanol–pentane as a solvent, and 18% of benzyl methyl ether is also formed under these conditions.<sup>1</sup>

The substantial trapping of carbene **1** in methanol/pentane raises the question of how alkoxychlorocarbenes fragment in hydrocarbon solvents because one would not expect ionic fragmentations to proceed in such media. To address this



question, we have to consider that carbene **1** can exist or be generated in two conformations (configurations), *cis*-**1** and *trans*-**1** whose fragmentation behavior may be quite different.<sup>8</sup>



Whereas in sufficiently polar solvents *trans*-**1** can cleave to form an ion pair (separated by a molecule of CO), *cis*-**1** may fragment via a tight ion pair<sup>9</sup> or, in the limit, by a *concerted* process where the incipient benzyl cation and chloride anion recombine to form benzyl chloride as CO is expelled. A corresponding transition state (Figure 1) was located in a previous computational study where the calculated activation energy for the fragmentation of *cis*-**1** in a vacuum was found to be only 6.7 kcal/mol,<sup>10</sup> so that this fragmentation should certainly occur at ambient temperature in pentane. Interestingly, the activation energy dropped to 1.45 kcal/mol in acetonitrile,<sup>10</sup> which indicates that the transition state is much more polar than the reactant carbene.

In the transition state of Figure 1,  $r_2$  is 3.35; a strong benzyl-C ( $\delta^+$ ) and chloride ( $\delta^-$ ) interaction clearly exists. The fragmentation is advanced at the cationic center, where the C-O separation ( $r_1$ ) is 2.20 Å and bond angles  $\alpha$  and  $\beta$  approach 120°.

On the other hand, the attraction between the nascent chloride anion and the benzyl cation is strongly attenuated by the intervening CO molecule in the transition state for the fragmentation of *trans*-**1** (see eq 3). However, according to SCI-PCM calculations,<sup>10</sup> the fragmentation of **1** to  $\text{PhCH}_2^+$ , CO, and  $\text{Cl}^-$  is slightly exothermic in acetonitrile (and, presumably also in methanol), so that the development of solvated ions from *trans*-**1** is conceivable under these conditions and may indeed account for the formation of  $\text{PhCH}_2\text{OMe}$  in MeOH.<sup>1</sup>

Due to lack of solvation for the developing ions, heterolytic fragmentation of *trans*-**1** in a vacuum (and, presumably, pentane) is energetically prohibitive ( $\Delta E_{\text{calc}} > 100$  kcal/mol<sup>10</sup>), but *homolytic* fragmentation ( $\Delta E_{\text{calc}} \sim 8.6$  kcal/mol) to give the benzyl radical and COCl (which itself loses CO quite easily) may become competitive with other processes in nonpolar solvents.

In the present report we examine the fragmentations of several representative alkoxychlorocarbenes in hydrocarbon solvents. We consider benzyloxychlorocarbene (**1**), cyclohexyloxychlorocarbene (**4**), and *n*-octyloxychlorocarbene (**5**) in MeCN, DCE, benzene, cyclohexane, or pentane.

Prior product and kinetics studies have appeared for the fragmentations of **1**<sup>4,5</sup> and *n*-butoxychlorocarbene (an analogue

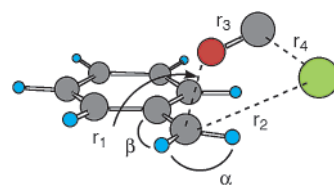
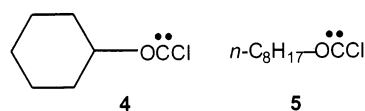


**Figure 1.** B3LYP/6-31G\* transition state for the gas-phase fragmentation of *cis*-**1**:  $r_1 = 2.200$ ;  $r_2 = 3.349$ ;  $r_3 = 1.173$ ;  $r_4 = 2.396$  (all distances in Å);  $\alpha = 118.5^\circ$ ;  $\beta = 120.3^\circ$ .

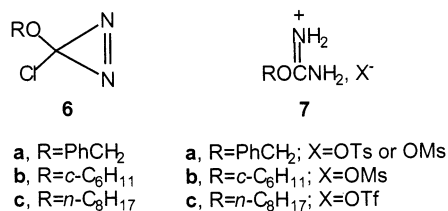
of **5**<sup>11</sup>), in polar solvents (MeCN, DCE). Here, we demonstrate for the first time the persistence of efficient fragmentation in



hydrocarbon solvents. Moreover, we extend studies of carbene **1** to Ar matrixes at 12 K, where we encounter reactive intermediates not readily observed in solution at ambient temperature. At the same time we extend the previous computational investigations on the fragmentations of oxychlorocarbenes<sup>10</sup> to provide a coherent framework for the interpretation of the new experimental findings that are presented in this work.

## Experimental Results and Discussion

**Reactions and Products.** Carbenes **1**, **4**, and **5** were generated by photolysis or thermolysis of 3-alkoxy-3-chlorodiazirines **6**, which were prepared by hypochlorite oxidation (Graham reaction)<sup>12</sup> of isouronium salts **7**. The latter were



synthesized from the appropriate alcohol, cyanamide, and strong acid (HX) by previously described methods.<sup>1,13</sup> Except for diazirine **6c**, these carbene precursors have been previously prepared and were characterized by their IR, UV, and NMR spectra.<sup>1,14</sup> All diazirines were purified before use by short-path chromatography over silica gel, with pentane elution. When experiments required alternative solvents, pentane was removed under reduced pressure and replaced by the solvent of choice. Photolysis ( $\lambda > 320$  nm) or thermolysis of diazirines **6** were carried out at 25 °C. Products were analyzed by GC and GC-MS and confirmed by spiking comparisons with authentic materials.

**Benzyloxychlorocarbene (1).** The fragmentation of carbene **1** in MeCN led to benzyl chloride and *N*-benzylacetamide, a "Ritter" product formed by the attack of the benzyl cation on MeCN, followed by hydrolysis with adventitious water.<sup>1,4</sup> In DCE, only benzyl chloride formed from the fragmentation of **1**.<sup>5</sup> These results, together with product distributions for the fragmentations of **1** in cyclohexane, benzene, and pentane, appear in Table 1.

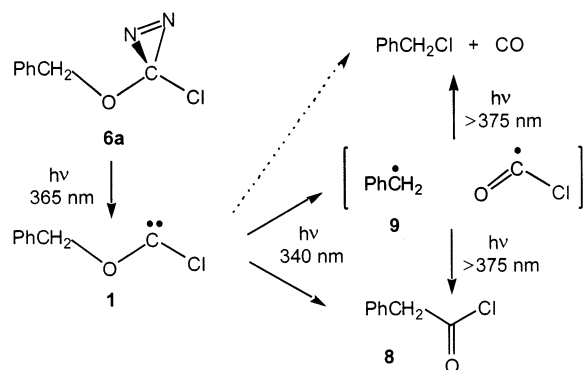
From Table 1, it is clear that quantitative or near quantitative fragmentation to benzyl chloride and CO is the principal fate of carbene **1** in MeCN, DCE, benzene, or pentane solutions at ambient temperature. Only in cyclohexane is there substantial side product formation. The cyclohexyl chloride and cyclohex-

**TABLE 1: Product Distributions (%) from Benzyloxy-chlorocarbene (1)<sup>a</sup>**

solvent	method <sup>b</sup>	PhCH <sub>2</sub> Cl	PhCH <sub>2</sub> NHCOMe	reference
MeCN	<i>hν</i>	63	37	4
DCE	<i>hν</i>	100		5
benzene	<i>hν</i>	100		<i>c</i>
cyclohexane	<i>hν</i>	80 <sup>d</sup>		<i>c</i>
pentane	<i>hν</i>	94 <sup>e</sup>		<i>c</i>
pentane	Δ	98 <sup>f</sup>		<i>c</i>

<sup>a</sup> All reactions at 25 °C; the absorbance of diazirine **6a** was 1.0 at  $\lambda_{\text{max}}$ . <sup>b</sup> Decomposition method for the diazirine. <sup>c</sup> This work. <sup>d</sup> 9% of cyclohexyl chloride and 11% of cyclohexanol also formed. <sup>e</sup> 3% of benzaldehyde and 2% of benzyl formate also formed. <sup>f</sup> 2% of benzaldehyde formed.

**SCHEME 1: Photolysis of Diazirine 6a in an Argon Matrix at 12 K**



anol may result from reaction pathways involving cyclohexyl and benzyl radicals. LFP<sup>1,15,16</sup> and matrix isolation experiments (see below) do indeed indicate minor benzyl radical formation (<10%) in the fragmentation of **1**. Note, however, that the only benzyl-containing product formed from carbene **1** in cyclohexane is the expected fragmentation product, PhCH<sub>2</sub>Cl, whereas toluene (the H-abstraction product expected from benzyl radical) is not observed.

In contrast, the most conspicuous product observed after 365 nm photolysis of diazirine **6a** embedded in an Ar matrix at 12 K is the benzyl radical with its signpost optical bands at 400–450 and 280–320 nm (see traces a and d in Figure 2). However, a featureless absorption extending from 260 to 360 nm indicates the presence of another species (carbene **1**) that can be bleached by >340 nm photolysis with the formation of more benzyl radical (Figure 2c). Finally, >375 nm irradiation leads to loss of the benzyl radical, which is accompanied by a partial recovery of the above 260–360 nm UV band. These results are shown in Scheme 1.

More detailed information is gained from the IR spectra shown in Figure 3. The difference spectrum (a) for the 365 nm photolysis of **6a** very clearly shows the rise of the prominent bands of CO (2143 cm<sup>-1</sup>), COCl (1870 cm<sup>-1</sup>), and phenacyl chloride **8** (1800–1820 cm<sup>-1</sup>). On subsequent bleaching at >375 nm (difference spectrum b), the COCl peaks and several bands that we attribute to the benzyl radical<sup>17</sup> decrease, whereas those of CO and phenacyl chloride increase (the latter very weakly). In addition, a group of bands attributed to benzyl chloride (by comparison with an authentic sample) also gain in intensity. On subsequent 340 nm irradiation (difference spectrum c, which corresponds to the bleaching of the broad UV band) the COCl and benzyl radical bands are partially recovered. Most of the IR peaks that decrease in this experiment can be attributed to the two conformers of benzyloxychlorocarbene **1** (cf., the

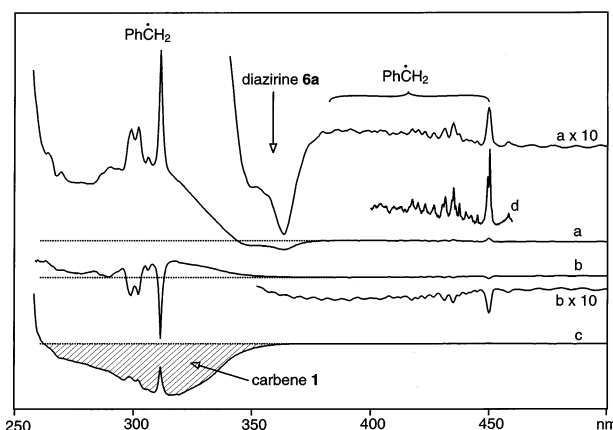


**Figure 2.** Difference UV-vis spectra obtained in an Ar matrix at 12 K: (a) after irradiation of diazirine **6a** at 365 nm; (b) after subsequent bleaching of the radical pair (PhCH<sub>2</sub>···COCl) at >375 nm; (c) after subsequent bleaching of carbene **1** at 340 nm; (d) high-resolution (0.1 nm) scan of the first band of benzyl radical, based on spectrum (a).

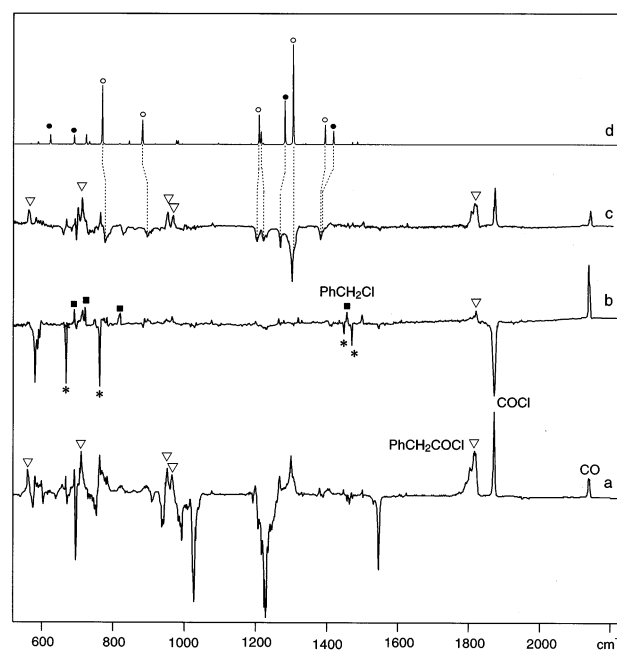


**Figure 3.** Difference IR spectra obtained in an Ar matrix at 12 K (a) after 365 nm irradiation of diazirine **6a**; (b) subsequent bleaching of the PhCH<sub>2</sub>···COCl radical pair at >375 nm; (c) bleaching of carbene **1** at 340 nm. Inverted triangles denote IR bands of phenacyl chloride, filled squares those of benzyl chloride, asterisks are for IR bands of benzyl radical; (d) spectrum of a 75:25 mixture of *trans*- (open circles) and *cis*-**1** (filled circles) calculated by B3LYP/6-31G\*.

calculated spectrum of a 75:25 mixture of the *anti*- and *syn*-conformers, Figure 3d).

By internal calibration experiments involving known quantities of the stable products (CO, benzyl chloride, phenacyl chloride), we are able to quantitate the yields of all the species obtained in the various photolyses using integrated IR band intensities (Table 2). From this it becomes evident that, despite their prominence in the UV/vis spectra (Figure 2), the radical cleavage products, benzyl and COCl, are minor products of the bleaching of diazirine **6a**. However, these products gain more prominence in the photolysis of carbene **1**.

The occurrence of phenacyl chloride **8** as a major product constitutes the chief difference between the room temperature solution experiments and those in Ar matrices at 12 K. LFP-TRIR experiments suggest the possible minor involvement of

TABLE 2: Results of Photolyses in Ar Matrixes at 12 K

reactant	irradiation wavelength (nm)	percent <sup>a</sup>	products
diazirine <b>6a</b>	365	46 ± 6 27 ± 5 20 ± 8 7 ± 2	PhCH <sub>2</sub> –COCl PhCH <sub>2</sub> –Cl + CO PhCH <sub>2</sub> –OCCl PhCH <sub>2</sub> • + COCl•
PhCH <sub>2</sub> •••COCl•	> 375	85 ± 3 15 ± 3	PhCH <sub>2</sub> –Cl + CO PhCH <sub>2</sub> –COCl
PhCH <sub>2</sub> OCCl	340	53 ± 5 33 ± 5 14 ± 2	PhCH <sub>2</sub> –COCl PhCH <sub>2</sub> • + COCl• PhCH <sub>2</sub> –Cl + CO
diazirine <b>6a</b>	(overall)	59 41	PhCH <sub>2</sub> –COCl PhCH <sub>2</sub> –Cl + CO

<sup>a</sup> Uncertainties arise mainly from the accuracy with which partial pressures of CO, PhCH<sub>2</sub>Cl, and PhCH<sub>2</sub>–COCl could be gauged in the calibration experiments. In the case of the carbene, overlapping bands caused additional difficulties. The quoted uncertainties are conservative estimates.

**8** during the LFP of **6a** in cyclohexane. The formation of **8** could be rationalized as a recombination product of the radical pair [9•••COCl] that is formed by homolytic scission of **1**. Interestingly, only 15% of **8** is formed in the photochemical bleaching of this radical pair; the main process is Cl abstraction by **9** from COCl, a reaction that is exothermic by 57 kcal/mol. Hence, any radicals that might be formed by homolytic cleavage of **1** in solution are likely to decay by this route. Alternatively, **8** could arise by direct 1,2 migration of benzyl from oxygen to the carbene center, a mechanism that is perhaps operative in the bleaching of **1**, which leads to over 50% of **8**. This mechanistic possibility will be examined by computational means below.

The general absence of phenacyl chloride (or products derived therefrom) in the solution LFP experiments is probably due to the fact that  $\Delta H_{298}$  for the dissociation of COCl is only about 8 kcal/mol.<sup>18a</sup> Hence, in contrast to the situation in a matrix at 12 K, the lifetime of COCl at room temperature may be too short to undergo efficient recombination with the benzyl radical to form **8**. However, the Cl radicals that remain after dissociation of COCl can easily recombine with **9** to form benzyl chloride or abstract hydrogen atoms from the solvent to form HCl, which may explain some of the other products that are isolated in the solution runs in cyclohexane (see Table 1).

Thus, the Ar matrix results suggest that benzyl chloride may form from **1** in pentane via different pathways, i.e., a concerted one from *cis*-**1**, or a sequential one from *trans*-**1**. Which pathway dominates will depend on the relative activation energies for the dissociation of *trans*-**1** to **9** and COCl and for the rotamerization to *cis*-**1** (which will promptly decay to benzyl chloride by “concerted” elimination of CO).

**Cyclohexyloxychlorocarbene (4).** Fragmentation of carbene **4** in MeCN or DCE mainly produces cyclohexyl chloride and cyclohexene, which can be rationalized by cation–anion recombination or “HCl” elimination by  $\beta$ -carbon-to-chloride proton transfer within an ion pair.<sup>19</sup> Product distributions appear in Table 3 for the fragmentations of carbene **4** in MeCN, DCE, benzene, and pentane.

Apart from the formation of 11% of cyclohexyldichloromethyl ether (the HCl-trapping product of carbene **4**) in benzene,<sup>20</sup> carbene fragmentation is the dominant fate of this *sec*-alkoxychlorocarbene in the hydrocarbon solvents benzene and pentane. Because ionic fragmentation is thermochemically impossible in these solvents (see computational part), concerted<sup>9</sup> or radical processes must account for the formation of the observed fragmentation products. The computational studies will

TABLE 3: Product Distributions (%) from Cyclohexyloxychlorocarbene (**4**)<sup>a</sup>

solvent	method <sup>b</sup>	<i>c</i> -C <sub>6</sub> H <sub>11</sub> Cl	cyclohexene	reference
MeCN	<i>hν</i>	62	32 <sup>c</sup>	14
DCE	<i>hν</i>	70	30	14
benzene	<i>hν</i>	53	36 <sup>d</sup>	<i>e</i>
pentane	<i>hν</i>	53	42 <sup>f</sup>	<i>e</i>
pentane	Δ	43	57	<i>e</i>

<sup>a</sup> All reactions at 25 °C; the absorbance of diazirine **6b** was 1.0 at  $\lambda_{\max}$ . <sup>b</sup> Decomposition method for the diazirine. <sup>c</sup> 6% of *N*-cyclohexylacetamide also formed. <sup>d</sup> 11% of cyclohexyl dichloromethyl ether formed. <sup>e</sup> This work. <sup>f</sup> 5% of an unidentified product was also present.

TABLE 4: Product Distributions (%) from *n*-Octyloxychlorocarbene (**5**)<sup>a</sup>

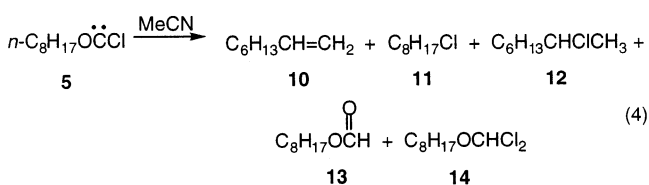
solvent	method <sup>b</sup>	1-octene	<i>n</i> -Oct-Cl	2-Oct-Cl	<i>n</i> -Oct formate	<i>n</i> -Oct OCHCl <sub>2</sub>
MeCN	<i>hν</i>	37	25	10	13	15
benzene <sup>c</sup>	<i>hν</i>	30	19	5	2	29
pentane <sup>d</sup>	<i>hν</i>	32	41	5	12	
pentane	Δ	39	55	6		

<sup>a</sup> At 25 °C; the absorbance of diazirine **6c** was 1.0 at  $\lambda_{\max}$ .

<sup>b</sup> Decomposition method for the diazirine. <sup>c</sup> 15% of another component, possibly an azine, was present. <sup>d</sup> 9% of an unknown component was present.

provide some insight as to the mechanism of these reactions in nonpolar solvents. We do not have an explanation for the apparent dependence of the cyclohexyl chloride/cyclohexene distribution in pentane on the method of carbene generation (Table 3), but both products arise by carbene fragmentation. As will be shown below, isolated ethoxychlorocarbene is predicted to undergo concerted elimination of CO and HCl with  $\Delta H^\ddagger = \sim 20$  kcal/mol and fragmentation with  $\Delta H^\ddagger = \sim 26$  kcal/mol.

***n*-Octyloxychlorocarbene (5).** Primary alkoxychlorocarbenes (RCH<sub>2</sub>OCCl, R = *n*-C<sub>4</sub>H<sub>9</sub> or *i*-C<sub>4</sub>H<sub>9</sub>) fragment in MeCN by bimolecular processes that involve S<sub>N</sub>2 attack of Cl<sup>−</sup> at the  $\alpha$ -methylene carbon atom of the carbene.<sup>11</sup> We examined carbene **5** to determine if a MeCN to hydrocarbon solvent change impeded carbene fragmentation. The products obtained from **5**, as generated by the photolysis of diazirine **8c** in MeCN, are shown in eq 4; product distributions appear in Table 4.



1-Octene (**10**), *n*-octyl chloride (**11**), and 2-chlorooctane (**12**) are fragmentation products of carbene **5**, whereas octyl formate (**13**) and *n*-octyl dichloromethyl ether (**14**) represent carbene trapping by water or HCl, respectively. The products are analogous to those observed from *n*-butoxychlorocarbene in MeCN,<sup>11</sup> although we did not detect carbene dimer or azine (see below). In MeCN, fragmentation of **5** accounts for  $\sim 72\%$  of the total product. Fragmentation (**10** + **11** + **12**) decreases to 53% in benzene, where about 15% of azine appears to form (on the basis of the MS fragmentation pattern of an additional product). In pentane, fragmentation accounts for 78–100% of the products, depending on the method of carbene generation. Clearly, fragmentation is not inhibited by a solvent change from polar MeCN to nonpolar pentane, even though ionic fragmentation should not occur in pentane.

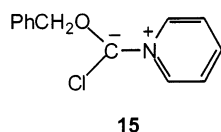


**TABLE 5: Rate Constants ( $k_{\text{frag}}$ ,  $\text{s}^{-1}$ ) for Fragmentations of  $\text{PhCH}_2\text{OCCl}$  (1)<sup>a</sup>**

method <sup>b</sup>	MeCN <sup>c</sup>	DCE <sup>c</sup>	benzene <sup>d</sup>	pentane <sup>d</sup>
UV–pyridine	$3.6 \times 10^5$	$6.2 \times 10^4$	$5.0 \times 10^5$	<i>e</i>
TRIR	$4.4 \times 10^5$	$2.9 \times 10^5$	<i>e</i>	$1.8 \times 10^5$

<sup>a</sup> At 25 °C. Errors in  $k_{\text{frag}}$  are 10–15%. <sup>b</sup> Monitoring method for the LFP experiments; see text. <sup>c</sup> Data from ref 5. <sup>d</sup> This work. <sup>e</sup> Not determined.

**Kinetics.** We determined rate constants for the fragmentations of carbenes **1** and **5** in various solvents. For carbene **1**, the rate constants were obtained by LFP, using both UV and TRIR monitoring methods.<sup>5</sup> LFP–UV studies were previously reported for carbene **1** in MeCN and DCE solvents;<sup>4,5</sup> the most recent values of  $k_{\text{frag}}$  are  $(3.6 \pm 0.45) \times 10^5 \text{ s}^{-1}$  (MeCN) and  $(6.2 \pm 0.2) \times 10^4 \text{ s}^{-1}$  (DCE).<sup>5</sup> We repeated these measurements in benzene, using the pyridine ylide method<sup>21</sup> to derive  $k_{\text{frag}}$ .<sup>4,5</sup> Thus, LFP of diazirine **6a** ( $A_{350} = 1.0$ ) with a xenon fluoride excimer laser<sup>22</sup> at 351 nm and 25 °C in benzene containing added pyridine produced an absorption at 412 nm due to ylide **15**.<sup>23</sup>



A correlation of the apparent rate constants for ylide formation ( $k_{\text{obs}}$ ,  $(1.2\text{--}2.5) \times 10^6 \text{ s}^{-1}$ ) vs pyridine concentration (2.47–7.42 M) was linear (7 points,  $r = 0.992$ ) with a slope of  $2.7 \times 10^5 \text{ M}^{-1} \text{ s}^{-1}$ , which can be taken as the second-order rate constant for ylide formation,  $k_y$ .<sup>21,24</sup> The *Y*-intercept at  $[\text{pyr}] = 0$  was  $5.5 \times 10^5 \text{ s}^{-1}$ , which represents the sum of the rate constants for all processes that destroy carbene **1** in the absence of pyridine. As indicated in Table 1,  $\text{PhCH}_2\text{OCCl}$  quantitatively fragments to benzyl chloride in benzene, so that  $5.5 \times 10^5 \text{ s}^{-1}$  is a good estimate of  $k_{\text{frag}}$ . Repetition of this determination led to  $k_{\text{frag}} = 4.5 \times 10^5 \text{ s}^{-1}$ , giving an average value of  $k_{\text{frag}} = (5.0 \pm 0.5) \times 10^5 \text{ s}^{-1}$ .<sup>25</sup> Rate constants for the fragmentation of carbene **1** appear in Table 5.

For comparison with previous determinations, we also measured  $k_{\text{frag}}$  for **1** in DCE using the UV–pyridine monitoring method. We obtained  $k_{\text{frag}} = (6.2 \pm 0.3) \times 10^4 \text{ s}^{-1}$ . The  $k_{\text{frag}}$  measurement is in excellent agreement with the earlier value  $[(6.2 \pm 0.2) \times 10^4 \text{ s}^{-1}]$ .<sup>5</sup> In DCE, fragmentation of carbene **1** to benzyl chloride is quantitative; cf., Table 1.

We were unable to determine  $k_{\text{frag}}$  for **1** in pentane (or cyclohexane) by the LFP–UV–pyridine method. The UV absorption of ylide **15** was very poor in these solvents and could not be exponentially fitted at lower  $[\text{pyr}]$ . Similar difficulties were encountered with carbene **4** in both benzene and pentane. Accordingly, we used the LFP–TRIR spectroscopy<sup>26</sup> to measure  $k_{\text{frag}}$  for carbene **1** in pentane. We monitored the time-dependent formation of CO at  $2120 \text{ cm}^{-1}$  by TRIR during the fragmentation of carbene **1** in pentane. Analysis of the growth of the CO over 9  $\mu\text{s}$  after the laser flash gave  $k = 1.84 \times 10^5 \text{ s}^{-1}$ ; cf., Table 5.

The TRIR-determined rate constants in Table 5 manifest small differences that may reflect the decreasing solvent polarity from MeCN to DCE to pentane. The UV–pyridine results, however, are not in a parallel sequence. To avoid overinterpretation of the data, we will not analyze small differences between  $k_{\text{frag}}$  values determined by different monitoring methods. The UV–pyridine and TRIR rate constants agree very well for ACN but

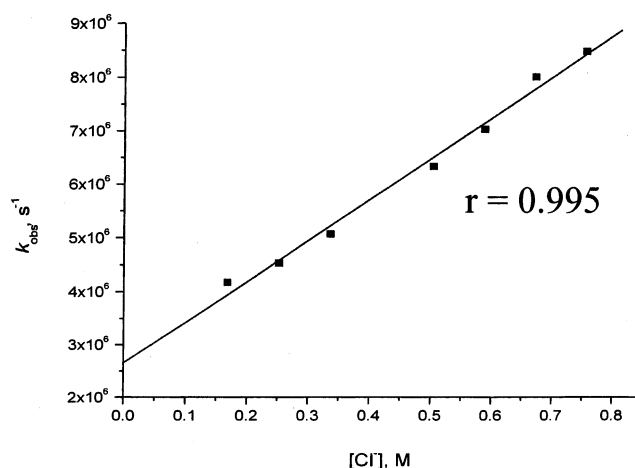
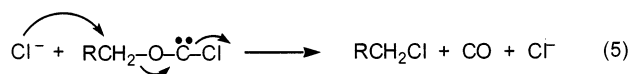


**Figure 4.** Correlation of  $k_{\text{obs}}$  ( $\text{s}^{-1}$ ) for the formation of the pyridinium ylide from carbene **5** and pyridine as a function of added  $\text{Bu}_4\text{NCl}$  (M) in 5.77 M pyridine–MeCN solutions at 25 °C. The slope of the correlation ( $k_2$ ) is  $1.2 \times 10^7 \text{ M}^{-1} \text{ s}^{-1}$ .

differ by a factor of 4.7 for DCE. This may be due to specific solvent effects of the pyridine probe, although the dielectric constants of pyridine and DCE are very similar. Suffice it to say that all the  $k_{\text{frag}}$  values are near  $10^5 \text{ s}^{-1}$ ; the fragmentations are fast and relatively independent of solvent, consistent with a very low activation energy for fragmentation, even in pentane.

We also measured  $k_{\text{frag}}$  for *n*-octyloxychlorocarbene (**5**) in MeCN and benzene. The rate constant for the analogous fragmentation of *n*-butyloxychlorocarbene in MeCN was previously determined as  $1.75 \times 10^6 \text{ s}^{-1}$  ( $E_a = 3.1 \text{ kcal/mol}$ ).<sup>11</sup> However,  $k_{\text{frag}}$  varied with added chloride, affording  $k_2 = 8.2 \times 10^6 \text{ M}^{-1} \text{ s}^{-1}$ , consistent with a “bimolecular” fragmentation induced by  $\text{S}_{\text{N}}2$  attack of  $\text{Cl}^-$  at the carbene’s  $\alpha$ -carbon that avoids a “unimolecular” fragmentation via a primary alkyl cation; cf., eq 5.<sup>11</sup>



With the UV–pyridine method, LFP studies of the fragmentation of **5** in MeCN gave  $k_{\text{frag}} = (1.6 \pm 0.03) \times 10^6 \text{ s}^{-1}$  (and  $k_y = (1.9 \pm 0.06) \times 10^5 \text{ M}^{-1} \text{ s}^{-1}$ ), in excellent agreement with the kinetic data for the fragmentation of *n*-BuOCCl in MeCN.<sup>11</sup> Measurement of  $k_{\text{frag}}$  for carbene **5** in benzene gave  $(5.1 \pm 0.3) \times 10^5 \text{ s}^{-1}$  and  $k_y = (2.5 \pm 0.04) \times 10^5 \text{ M}^{-1} \text{ s}^{-1}$ .

The bimolecular fragmentation mechanism of eq 5 was verified for the decomposition of carbene **5** in MeCN. LFP of diazirine **6c** in MeCN solutions containing a constant concentration of pyridine (5.77 M) and varying quantities of tetra-*n*-butylammonium chloride (0.17–0.76 M) gave a linear ( $r = 0.995$ ) correlation of  $k_{\text{obs}}$  for the formation of ylide vs  $[\text{Cl}^-]$ , affording  $k_2 = 1.2 \times 10^7 \text{ M}^{-1} \text{ s}^{-1}$ ; cf., Figure 4.<sup>27</sup> This value is in good agreement with the analogous rate constant for the chloride-induced fragmentation of *n*-BuOCCl in MeCN ( $8.2 \times 10^6 \text{ M}^{-1} \text{ s}^{-1}$ ).<sup>11</sup>

The foregoing experiments support the contention that neither the product distribution nor the fragmentation rate constants are greatly altered by solvent variation between MeCN, DCE, benzene, and pentane. This is surprising in view of the  $\sim 5.2 \text{ kcal/mol}$  computed reduction of activation energy for the fragmentation of  $\text{PhCH}_2\text{OCCl}$  in MeCN vs vacuum (and, presumably pentane); see above.<sup>10</sup>

**TABLE 6: Geometry Parameters,<sup>a</sup> Relative Energies (kcal/mol), and Partial Charges of CH<sub>3</sub>OCCl Isomers and Transition States in the Gas Phase and in Simulated CH<sub>3</sub>CN (SCI-PCM)**

	<i>trans</i> -carbene		<i>cis</i> -carbene		fragmentation TS <sup>b</sup>		<i>cis</i> – <i>trans</i> -isom TS		rearrangement TS <sup>c</sup>	
	gas phase	CH <sub>3</sub> CN	gas phase	CH <sub>3</sub> CN	gas phase	CH <sub>3</sub> CN	gas phase	CH <sub>3</sub> CN	gas phase	CH <sub>3</sub> CN
H <sub>3</sub> C–O	1.453 Å	1.466 Å	1.468 Å	1.478 Å	2.185 Å	2.181 Å	1.446 Å	1.470 Å	1.796 Å	1.918 Å
O–C	1.296 Å	1.280 Å	1.278 Å	1.264 Å	1.176 Å	1.160 Å	1.289 Å	1.225 Å	1.246 Å	1.200 Å
C–Cl	1.809 Å	1.848 Å	1.872 Å	1.904 Å	2.337 Å	2.624 Å	1.898 Å	2.119 Å	1.946 Å	2.213 Å
H <sub>3</sub> C...Cl	3.882 Å	3.924 Å	2.941 Å	2.981 Å	2.795 Å	2.968 Å	3.513 Å	3.875 Å	3.326 Å	3.490 Å
H <sub>3</sub> C–O–C	114.9°	115.9°	129.1°	130.2°	122.8°	129.6°	125.6°	146.8°	74.8°	77.1°
O–C–Cl	105.3°	105.0°	111.1°	111.3°	99.8°	95.9°	107.1°	106.6°	111.8°	110.3°
H <sub>3</sub> C–O–C–Cl	180.0°	180.0°	–0.02°	–0.01°	0.0°	0.22°	95.7°	105.6°	114.1°	105.0°
B3LYP/6-31G*	(0) <sup>g</sup>	(0) <sup>h</sup>	+0.93	+0.58	+37.26	+30.60	+18.11	+15.90	+40.46	+36.00
CCSD(T)/DZ <sup>d</sup>	(0)		+1.06		+38.17		+20.89		+43.90	
CCSD(T)/TZ <sup>e</sup>	(0)		+1.66		+42.26		+20.88		+43.14	
ZPE (B3LYP)	29.28	29.12	29.22	29.12	26.07	25.87	28.47	28.10	27.36	26.79
δ(Cl) <sup>f</sup>	–0.087	–0.151	–0.133	–0.191	–0.394	–0.656	–0.165	–0.425	–0.246	–0.532
δ(OC) <sup>f</sup>	–0.202	–0.241	–0.173	–0.160	–0.034	+0.025	–0.106	+0.094	–0.046	+0.019
δ(CH <sub>3</sub> ) <sup>f</sup>	+0.289	+0.392	+0.306	+0.351	+0.428	+0.631	+0.271	+0.331	+0.292	+0.513

<sup>a</sup> For structures see Figure 6. <sup>b</sup> TS for loss of CO and concomitant formation of CH<sub>3</sub>Cl. <sup>c</sup> TS for concerted CH<sub>3</sub>OCCl → CH<sub>3</sub>COCl rearrangement. <sup>d</sup> Single-point calculation with Dunning's cc-pVDZ basis set at the B3LYP geometry. Total energy: –612.40737 h. <sup>e</sup> Single-point calculation with Dunning's cc-pVTZ basis set at the B3LYP geometry. Total energy: –612.63992 h. <sup>f</sup> CHelpG charges for the indicated fragments. <sup>g</sup> Total energy: –613.34568 h. <sup>h</sup> Total energy: –613.351974 h.

## Computational Results and Discussion

**Previous Studies.** Several recent computational studies deal with the thermochemistry and the kinetics of the fragmentation of oxychlorocarbenes.<sup>10,19,28</sup> However, these studies focused on alkoxychlorocarbene fragmentations in polar solvents where fragmentation is presumed to lead to ion pairs. The same cannot happen in nonpolar solvents such as pentane or cyclohexane (benzene may stabilize ions through  $\pi$  donor/acceptor interactions in certain cases). In view of the present experimental findings we set out to examine in more detail processes that may contribute to the decay of alkoxychlorocarbenes RCH<sub>2</sub>OCCl under conditions where solvation is ineffective, and to examine the changes that are then brought about by introducing dielectric stabilization of the reacting species.

The previous studies have demonstrated that the activation barriers for the loss of CO from *cis*-carbenes (via transition states such as the one depicted in Figure 1) depend strongly on the nature of R and the presence or absence of a polar solvent, whereas the rotational barriers for interconversion of *cis*- and *trans*-carbenes are rather independent of these factors.

**Methoxychlorocarbene.** We started our investigation with methoxychlorocarbene, **16**, the smallest member of the series, because it is amenable to very high-level calculations, which allow us to assess the performance of the more economical B3LYP/6-31G\* method that will be used subsequently. The results of this study are given in Table 6 and Figure 5 which illustrate the following scenario: the *cis*- and *trans*-conformers of **16** are predicted to interconvert prior to any decomposition. The lowest energy dissociation pathway is straight homolytic cleavage of either conformer to •CH<sub>3</sub> + •COCl for which 18–22 kcal/mol are required at 0 K (zero-point energy differences calculated by B3LYP included). Interestingly the B3LYP/6-31G\* energy difference for this process is closer to that obtained at the CCSD(T) level with the triple- $\zeta$  than at the same level with a double- $\zeta$  basis set.

Experimentally, the dissociation enthalpy of •COCl is about 8 kcal/mol<sup>18</sup> so this energy must be added to arrive at •CH<sub>3</sub> + CO + •Cl.<sup>29</sup> Due to the high ionization energy of •CH<sub>3</sub>, heterolytic dissociation of **16** is of course prohibitively expensive in the gas phase, and although it is predicted to drop to 44.4 kcal/mol in MeCN, this process is not competitive with homolytic cleavage, even in this highly polar solvent.

If more energy becomes available, the next process that comes to the fore is the concerted elimination of CO and formation of

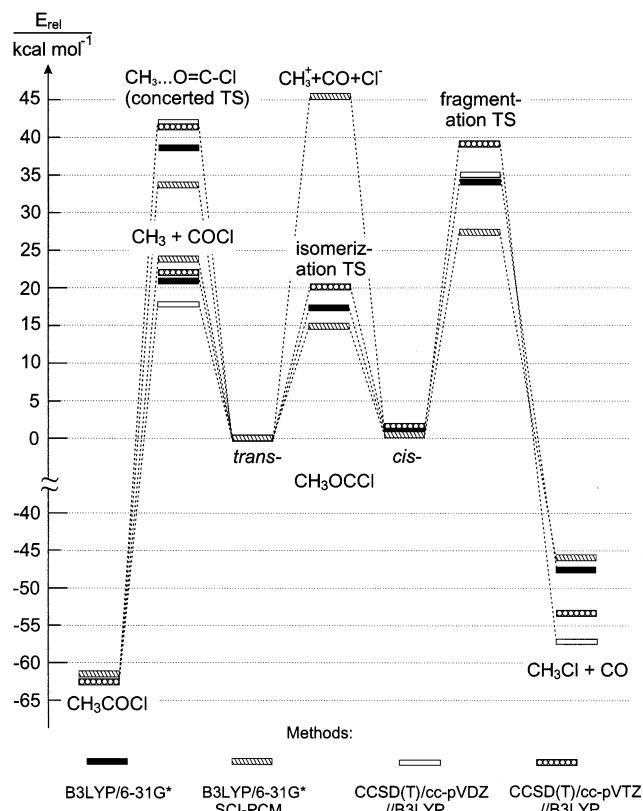


**Figure 5.** Energies of CH<sub>3</sub>OCCl and products of rearrangement and fragmentation by different methods relative to the *trans*-carbene.

CH<sub>3</sub>Cl whose gas-phase 0 K activation energy varies between ca. 34 (B3LYP) and 39 kcal/mol (CCSD(T)/cc-pVTZ at the B3LYP geometry ZPE differences included). It seems that B3LYP/6-31G\* underestimates the activation energy for this process, a feature that we will have to keep in mind when we interpret the results of these calculations for larger molecules. On going to acetonitrile, the barrier for this process is lowered by ca. 6.7 kcal/mol at the B3LYP level, which is easily understandable in view of the high degree of charge separation between the CH<sub>3</sub> and the COCl moieties that prevails at the transition state (cf., Table 6). We were surprised to note by how much the predictions of the different methods varied with regard to the energy liberated in the formation of MeCl + CO, and

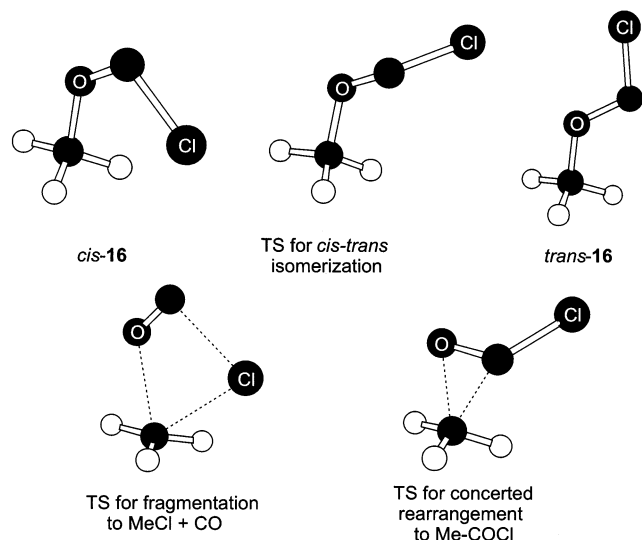


Figure 6. Structures of  $\text{CH}_3\text{OCCl}$  and corresponding species.

also how much this result depends on the basis set in the CCSD(T) calculations (cf., Table 6). Conversely, solvation by MeCN does not affect the exothermicity of this process very much.

We were also interested in the possibility of a concerted process leading from **16** to the much more stable isomeric acetyl chloride (a process that amounts to a 1,2-O–C methyl shift). Despite the strong exothermicity of this process, the corresponding transition state was found to lie 18–24 kcal/mol above the dissociation limit of **16** on a 0 K enthalpy scale. Again, we note that the B3LYP results are closer to those obtained at the CCSD(T) level with the triple- $\zeta$  than with the double- $\zeta$  basis set. However, all methods agree in predicting that the formation of alkanoyl chlorides from alkoxychlorocarbenes requires dissociation and recombination, even in polar solvents where the transition state for the concerted rearrangement is strongly stabilized due to the strong charge separation that also prevails in this geometry (cf., Figure 6)

In the case of  $\text{MeOCCl}$  and its products, all structures were fully reoptimized with B3LYP in MeCN, using the SCI-PCM method, for which gradients are available. As can be seen from Table 6, the geometries of most equilibrium structures did not change very much on solvation, whereas those of the transition states are more strongly affected. The main change is invariably a lengthening of the C–Cl bond, which attains nearly 0.3 Å in the (very polar) fragmentation transition state. The reason for this is that the partial negative charge on Cl increases from 0.25 to 0.53 on going from the gas phase to MeCN, which results in the observed 7 kcal/mol differential stabilization of the transition state. A similar increase in the polarity of the transition state for *cis*→*trans* isomerization (charge on Cl goes from –0.165 to –0.425) leads to a similar effect, and a significant stabilization of the transition state by solvation. Notable also is the finding that the nonbonded  $\text{H}_3\text{C}\cdots\text{Cl}$  distance decreases significantly on going from the *cis*-carbene to the transition state for loss of CO in the gas phase, whereas in MeCN it remains almost the same. Thus, in solution, the tendency for the Cl atom to bond to the carbon center is attenuated.

**Ethoxychlorocarbene.** The finding that olefins are prominent products after decomposition of diazirines **6b** and **6c** led us to investigate possible pathways that would account for their formation. As a model system we chose ethoxychlorocarbene, **17** ( $\text{CH}_3\text{CH}_2\text{OCCl}$ ), whose potential surface is depicted schematically in Figure 7, on the basis of the data presented in Table

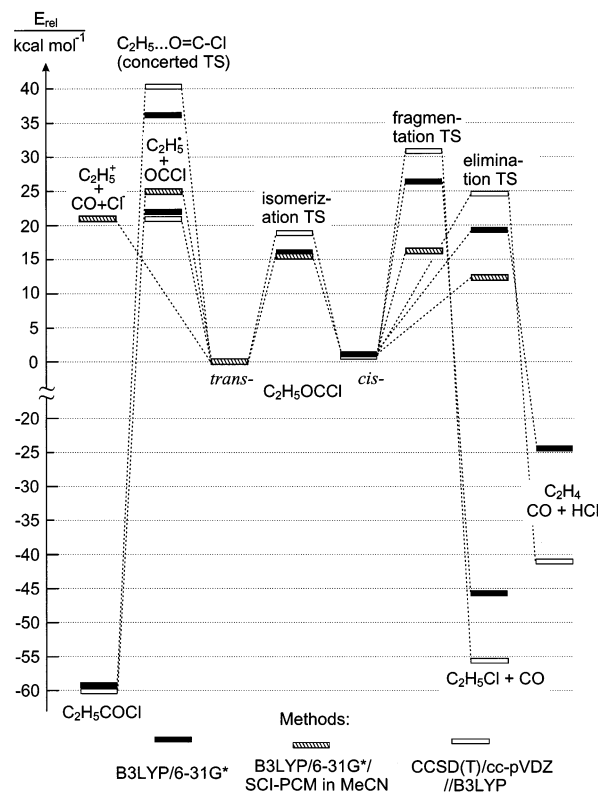


Figure 7. Energies of  $\text{CH}_3\text{CH}_2\text{OCCl}$  and products of rearrangement and fragmentation by different methods relative to the *trans*-carbene.

7. The energy difference between the *cis* and *trans* conformers does not differ much from the values found for  $\text{CH}_3\text{OCCl}$ , whereas the presence of the additional methylene group lowers the 0 K barrier for their interconversion by about 1.3 kcal/mol. In contrast, the activation barrier for concerted elimination of CO and formation of R–Cl decreases by 4–8 kcal/mol, although it is still higher than the barrier for *cis* → *trans* isomerization.

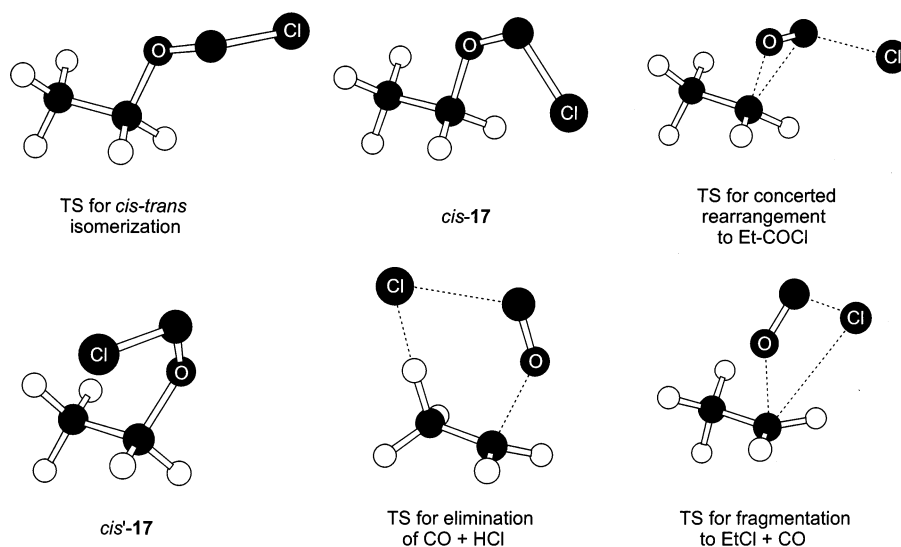
Most importantly, in our search for the transition state for the fragmentation process, we found another saddle point that was shown by IRC calculations to be connected adiabatically to ethene, CO, and HCl on the product side, and to a different *cis*-conformer of **17** on the reactant side (see Figure 8 for pictorial representations of the relevant geometries). The activation energy for this concerted elimination of CO and HCl was found to be 6–7 kcal/mol lower than that for fragmentation to  $\text{CO} + \text{C}_2\text{H}_5\text{Cl}$  so the two processes are likely to be competitive, in accord with the experimental findings for the two alkoxychlorocarbenes **4** and **5**, given the differing substitution patterns.

The energy for homolytic dissociation to  $\text{R}^\bullet + \cdot\text{COCl}$  is also slightly lowered by the additional methyl group in **17**, so that this process is again predicted to be competitive with the concerted eliminations described above. Different methods of calculations differ in the ordering of the energies for the three transition states: B3LYP/6-31G\* predicts elimination of  $\text{CO} + \text{HCl}$  to be favored by 3.6 kcal/mol over homolytic cleavage and by 5.8 kcal/mol over fragmentation to  $\text{CO} + \text{C}_2\text{H}_5\text{Cl}$ , whereas CCSD(T) calculations favor homolytic cleavage by 3 kcal/mol over elimination of  $\text{CO} + \text{HCl}$ . The same may also be true for the 1-octyl and cyclohexyl systems investigated experimentally, so that HCl might also arise by abstraction of a H atom  $\beta$  to the alkyl radical center by a Cl radical in nonpolar solvents, although we find no product evidence for extensive radical chain processes.

TABLE 7: Geometry Parameters,<sup>a</sup> Energies (kcal/mol), and Partial Charges of C<sub>2</sub>H<sub>5</sub>OCCl Isomers and Transition States

	<i>trans</i> -carbene	<i>cis</i> -carbene	fragmentation TS <sup>b</sup>	<i>cis</i> → <i>trans</i> -isom TS	elimination TS <sup>c</sup>	rearrangement TS <sup>d</sup>
CH <sub>2</sub> —O	1.469 Å	1.487 Å	2.278 Å	1.467 Å	1.976 Å	1.884 Å
O—C	1.293 Å	1.274 Å	1.169 Å	1.284 Å	1.182 Å	1.230 Å
C—Cl	1.815 Å	1.882 Å	2.459 Å	1.912 Å	2.392 Å	2.018 Å
CH <sub>2</sub> ...Cl	3.902 Å	2.968 Å	3.003 Å	3.543 Å	3.694 Å	3.337 Å
H <sub>2</sub> C—O—C	114.89°	129.84°	124.82°	126.11°	138.19°	77.06°
CH <sub>3</sub> —CH <sub>2</sub> —O—C	−112.32°	180.00°	−93.00°	168.96°	18.58°	−96.45°
O—C—Cl	105.38°	111.10°	101.31°	107.11°	112.51°	111.33°
CH <sub>2</sub> —O—C—Cl	179.20°	0.00°	−2.95°	96.11°	10.36°	−105.61°
B3LYP/6-31G*	(0) <sup>f</sup>	1.02	30.00	17.91	22.63	38.53
B3LYP/6-31G*/SCI-PCM	(0) <sup>g</sup>	0.71	19.75	16.41	15.57	33.89
CCSD(T)/cc-pVDZ <sup>e</sup>	(0) <sup>h</sup>	1.20	34.37	20.94	27.93	42.59
ZPE (B3LYP)	47.24	47.08	43.67	46.34	43.94	44.97
δ(Cl) <sup>i</sup>	−0.098/−0.177	−0.156/−0.183	−0.497/−0.633	−0.186/−0.232	−0.458/−0.593	−0.332/−0.415
δ(OC) <sup>i</sup>	−0.214/−0.176	−0.186/−0.197	−0.046/−0.059	−0.079/−0.074	−0.024/−0.027	−0.048/−0.056
δ(CH <sub>2</sub> ) <sup>i</sup>	+0.376/+0.401	+0.472/+0.507	+0.413/+0.577	+0.314/+0.434	+0.331/+0.456	+0.244/+0.315

<sup>a</sup> For structures see Figure 6. <sup>b</sup> Transition state for loss of CO and concomitant formation of EtCl. <sup>c</sup> Transition state for simultaneous loss of CO + HCl, formation of ethylene. <sup>d</sup> Transition state for concerted Et-OCCl → Et-COCl rearrangement. <sup>e</sup> Single point at B3LYP/6-31G\* geometry. <sup>f</sup> Total energy: −652.666125 h. <sup>g</sup> Total energy: −652.672248 h. <sup>h</sup> Total energy: −651.611325 h. <sup>i</sup> CHelpG charge on the fragments (in vacuo/in acetonitrile).

Figure 8. Structures of CH<sub>3</sub>CH<sub>2</sub>OCCl and corresponding species.

Due to homoconjugative stabilization of the incipient carbonium ion, the added methyl group assists the process of heterolytic cleavage to give R<sup>+</sup>, CO, and Cl<sup>−</sup> <sup>30</sup> even more than the above homolytic cleavage, although the energy for formation of ions remains prohibitively high in the gas phase. However, in acetonitrile, the energy of this assemblage of ions relative to the *trans*-carbene falls to 22 kcal/mol, so that heterolytic cleavage may indeed become competitive with homolytic fragmentation in acetonitrile even for primary alkoxychlorocarbenes. However, because the barriers for the concerted processes described above are also lowered significantly by solvation (see hashed bars in Figure 7), these processes are still predicted to dominate, even in MeCN, at least in **17**.

Hence the *trans*-carbene would rather isomerize to the *cis*-carbene than to undergo fragmentation and the *cis*-carbene prefers concerted loss of CO + HCl over elimination of CO alone, both in the gas phase and in polar solvents. Thus our calculations predict a change of mechanism on going from nonpolar solvents where the two conformers of the alkoxychlorocarbene interconvert prior to any fragmentation to polar solvents where these processes are at least competitive. As in the case of **16**, formation of propanoyl chloride (EtCOCl) requires homolytic cleavage and recombination of the fragments, because the transition state for concerted rearrangement lies significantly higher than the dissociation limit.

**Benzyloxychlorocarbene.** Finally, we repeated the above calculations for PhCH<sub>2</sub>OCCl (**1**), which stands at the focus of the present experimental investigation, and for which the greatest amount of experimental data are available. This study revealed some interesting new features that are highlighted in Figures 9 (on the basis of the data in Table 8) and 10. Unsurprisingly, the benzyl substituent leads to a substantial stabilization of the products of both homolytic and heterolytic ROCCl fragmentation. In fact, the latter process is even predicted to be slightly exothermic in acetonitrile (in DCjE it is calculated to be endothermic by 6.8 kcal/mol), thus supporting the idea that the formation of ions is likely an important process in polar solvents,<sup>3</sup> although the pyridine ylide carbene-trapping experiments indicate that heterolytic cleavage cannot be activationless, even in acetonitrile.

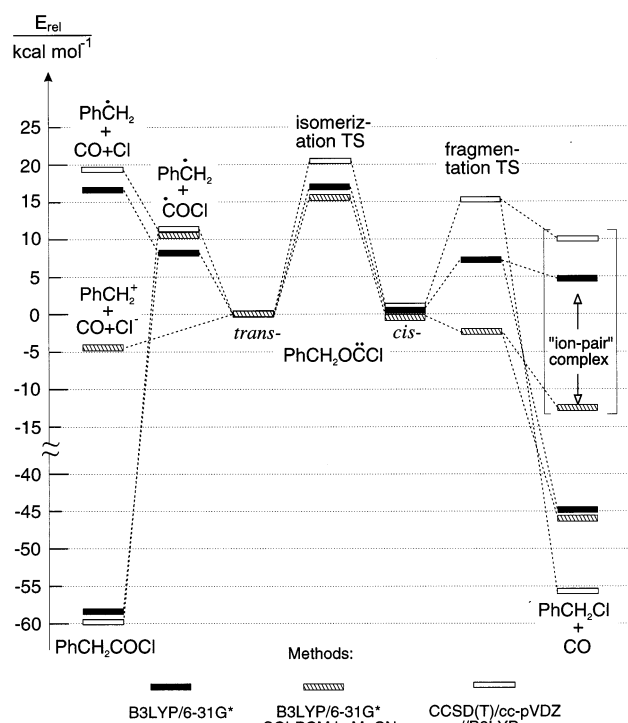
The activation barrier for *cis* → *trans* isomerization of the carbene remains essentially unaffected by the benzyl substituent. In contrast, the barrier for loss of CO decreases to ca. 7 (B3LYP) or 15 kcal/mol (CCSD(T)), respectively, whereas single point SCI-PCM calculations in MeCN at the B3LYP gas-phase geometry of the transition state even place this 2.4 kcal/mol below the starting *cis*-carbene.<sup>31</sup> This implies that the transition state for loss of CO lies much earlier on the reaction coordinate in the presence of MeCN; i.e., the gas-phase geometry of that transition state represents a point well beyond the transition state



**TABLE 8: Important Geometry Parameters,<sup>a</sup> Energies (kcal/mol), and Partial Charges of PhCH<sub>2</sub>OCCl, 1, Isomers and Transition States for Fragmentation and Isomerization**

	<i>trans</i> -carbene (C <sub>1</sub> )	<i>cis</i> -carbene (C <sub>2</sub> )	isomerization TS <sup>c</sup> (C <sub>1</sub> )	fragmentation TS <sup>b</sup> (C <sub>1</sub> )
H <sub>2</sub> C–O	1.481 Å	1.510 Å	1.486 Å	2.204 Å
O–C	1.292 Å	1.270 Å	1.281 Å	1.173 Å
C–Cl	1.815 Å	1.890 Å	1.923 Å	2.397 Å
H <sub>2</sub> C...Cl	3.911 Å	2.975 Å	3.558 Å	3.350 Å
H <sub>2</sub> C–O–C	114.52°	129.33°	125.03°	127.03°
C <sub>5</sub> H <sub>5</sub> –C–CH <sub>2</sub> –O	110.20°	108.11°	109.05°	107.05°
O–C–Cl	105.43°	111.40°	107.15°	109.83°
H <sub>2</sub> C–O–C–Cl	179.27°	0.00°	96.46°	0.58°
C–CH <sub>2</sub> –O–C	–109.23°	180.0°	167.66°	94.64°
B3LYP/6-31G*	(0) <sup>g</sup>	0.78	17.96	9.34
B3LYP/SCI-PCM <sup>d</sup>	(0)	–0.13	16.57	–0.20
MP2/6-31G* <sup>e</sup>	(0)	2.26	22.53	18.89
CCSD(T)/cc-pVDZ/	(0)	1.35	21.46	17.39
ZPE	80.52	80.21	79.51	78.35
δ(Cl) <sup>h</sup>	–0.110/–0.139	–0.168/–0.259	–0.200/–0.244	–0.510/–0.668
δ(O) <sup>h</sup>	–0.180/–0.181	–0.175/–0.131	–0.103/–0.105	–0.048/–0.084
δ(CH <sub>2</sub> ) <sup>h</sup>	+0.317/+0.340	+0.431/+0.416	+0.329/+0.378	+0.198/+0.282

<sup>a</sup> For structures see Figure 10. <sup>b</sup> TS for loss of CO and concomitant formation of PhCH<sub>2</sub>Cl. <sup>c</sup> TS for *cis* → *trans* isomerization. <sup>d</sup> Single point calculation at gas-phase B3LYP geometry, Total energy for *trans*-1: –844.406137 h. <sup>e</sup> At MP2/6-31G\* optimized geometries, total energy for *trans*-1: –842.589978 h. <sup>f</sup> Single point calculation at B3LYP geometry, total energy for *trans*-1: –842.809607 h. <sup>g</sup> Total energy: –844.399623 h. <sup>h</sup> CHelpG charges for the fragments (in vacuo/in CH<sub>3</sub>CN).

**Figure 9.** Energies of PhCH<sub>2</sub>OCCl and products of rearrangement and fragmentation by different methods relative to the *trans*-carbene.

in MeCN, which may explain why it lies below *cis*-1 in that solvent. Clearly, the geometry of this very polar (and in MeCN even more polar) transition state will be quite strongly affected by the presence of the solvent. Because we were unable to locate the transition state in acetonitrile, we cannot provide a prediction for the activation barrier for the elimination of CO in this solvent. However, we were able to confirm that the starting *cis*-carbene still represents a minimum on the B3LYP/SCI-PCM potential energy surface, so that this species is expected to have a finite lifetime even in polar solvents.

We have no explanation for the substantial discrepancy of the predictions made by the B3LYP and the CCSD(T) methods for the activation energies of this process. Apparently, the presence of the benzyl group's  $\pi$  system increases the contribution of dynamic electron correlation to the point where its

subtle changes on going from ground to transition states cannot be modeled accurately by either of the procedures at our disposition.

In any event, all methods agree in predicting that the *trans*-carbene would rather undergo cleavage to benzyl + COCl (homolytic in nonpolar, heterolytic in polar solvents<sup>30</sup>) than to isomerize to the *cis*-carbene, whereas the latter conformer is depleted by loss of CO in a process that will have a very small activation barrier in polar solvents.

In a next step we investigated the fate of *cis*-1 after it has crossed the transition state for loss of CO. In the cases of the methyl and ethyl derivatives, discussed above, IRC calculations had indicated that the decay leads directly to the corresponding alkyl chlorides. In the case of **1**, the situation turned out to be more complicated in that the IRC procedure (which amounts to an infinitely damped decay along the bottom of a potential valley leading from a transition state to a product) led to a structure, slightly below the transition state, where the Cl atom has moved into the plane of the benzyl moiety, bonded to two hydrogens, as indicated in Figure 10. At this point the CO had withdrawn so far from the PhCH<sub>2</sub>...Cl complex that gradients became too small for the IRC procedure to continue.

Removal of the CO and reoptimization of the remaining complex led to a stationary point that turned out to be a transition state in the gas phase that decays spontaneously to benzyl chloride upon the slightest twisting of the benzylic CH<sub>2</sub> group or displacement of the Cl atom out of the plane. This complex shows an unusually high degree of charge separation (Chelpg charge of –0.67 on Cl), which indicates a strong ion-pair nature, even in the gas phase. However, in the isolated species, this feature turned out to be artifactual and due to the imposed constraint of a closed-shell wave function. When this constraint was removed, the energy dropped by 1.5 kcal/mol and the species adopted partial triplet character ( $\langle S^2 \rangle$  increased to a value of 0.37) and the charge on Cl fell to –0.50. Concomitantly, a negative spin of 0.33 appeared on the Cl atom, balanced by a positive spin of the same magnitude in the  $\pi$  system of the benzyl moiety. These results indicate that the above complex has a high biradical character and that the lowest triplet and closed-shell singlet surfaces are in very close proximity.<sup>32</sup>

A polar solvent can of course again change the situation. Indeed, reoptimization of the above complex in acetonitrile by

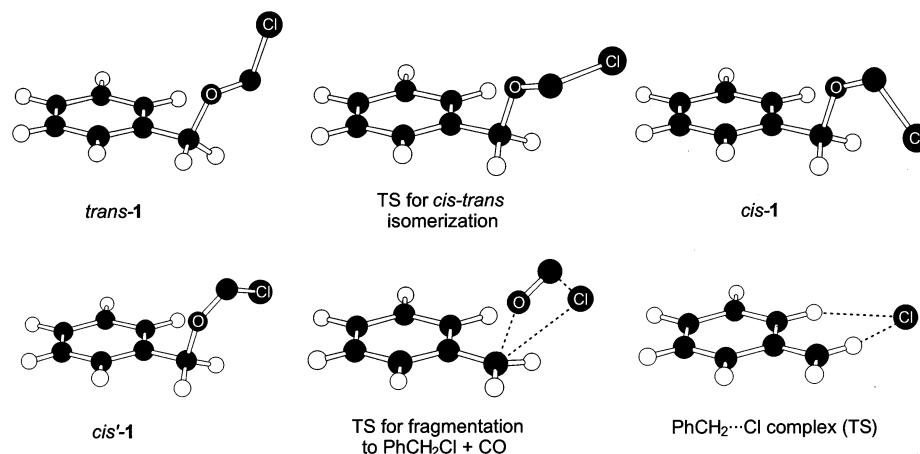


Figure 10. Structures of  $\text{PhCH}_2\text{OCCl}$  and resulting species.

B3LYP/SCI-PCM led to a potential energy minimum where the charge on Cl had increased to 0.90. We have not been able to find a transition state for the decay of this species to benzyl chloride, but our calculations seem to indicate that a tight benzyl-chloride ion pair may indeed have a fleeting existence in polar solvents (note that this species lies about 8 kcal/mol below the separated ions in acetonitrile, ca. 4 kcal/mol in dichloroethane), in contrast to nonpolar solvents where the corresponding biradicaloid does not represent a minimum on the potential surface.

All efforts to locate the transition state for concerted rearrangement of **1** to **8** failed, because in the presence of the phenyl substituent the degree of negative charge that accumulated on the COCl moiety near this transition state was high enough to provoke spontaneous loss of Cl from that fragment.<sup>30</sup> (In the gas phase collapse to benzyl chloride + CO ensued.) However, the fact that the activation barrier for concerted formation of RCOCl barely changed on going from  $\text{CH}_3\text{OCCl}$  to  $\text{C}_2\text{H}_5\text{OCCl}$  indicates that its energy relative to **1** is not very sensitive to substitution, from which we conclude that, if it exists, it must also lie well above the dissociation limit in the case of **1**. Hence, formation of **8** requires dissociation, and because heterolytic cleavage of **1** leads directly to  $\text{CO} + \text{Cl}^-$ ,<sup>30</sup> **8** will have no chance of forming in polar solvents. Even in nonpolar solvents, the COCl radical probably does not have a sufficient lifetime at room temperature to recombine with the benzyl radical to form **8** before it falls apart to  $\text{CO} + \text{Cl}$ , which explains the absence of this species from the TRIR experiments. In contrast, COCl persists in Ar matrixes and can reorient and recombine with the benzyl radical, in part after photoactivation of the latter.

As in the previous cases, we were dismayed to note the large discrepancies between the exothermicities predicted for the fragmentation to  $\text{RCl} + \text{CO}$  by the B3LYP and the CCSD(T) methods. Although we do not think that these discrepancies affect our conclusions, it might be worthwhile to investigate their causes.

## Conclusions

The calculations described above lead us to the following conclusions:

(a) Alkoxychlorocarbenes in the gas phase or in nonpolar solvents undergo rapid cis-trans rotamerization at room temperature ( $E_a = 16\text{--}18$  kcal/mol) before any fragmentation can intervene. Homolytic cleavage of the *trans*-carbene and concerted loss of  $\text{CO} + \text{HCl}$  from the *cis*-carbene are predicted to be competitive ( $E_a = 20\text{--}25$  kcal/mol), whereas loss of CO to

give alkyl chlorides requires ca. 6 kcal/mol more activation energy. At room temperature the COCl radicals formed by homolytic cleavage will rapidly dissociate to  $\text{CO} + \text{Cl}^\bullet$  ( $\Delta H = 8$  kcal/mol,  $\Delta G$  close to zero)<sup>18</sup> and recombination of the Cl with the alkyl radical will also lead to alkyl chlorides. Thus, the main products expected from fragmentation of alkoxychlorocarbenes in nonpolar solvents are alkyl chlorides and alkenes, in accord with experiment.

In polar solvents the two fragmentation transition states for  $\text{CH}_3\text{OCCl}$  and  $\text{C}_2\text{H}_5\text{OCCl}$  are stabilized to the point where cis-trans isomerization, loss of CO, and concerted loss of  $\text{CO} + \text{Cl}$  all have similar activation energies. Our calculations yield no indication that ion pairs intervene in these two fragmentation processes; i.e., loss of CO leads directly to alkyl chlorides. In acetonitrile, heterolytic cleavage becomes about 4 kcal/mol more favorable than homolytic cleavage but still requires 5–8 kcal/mol more energy than the above concerted processes (if heterolysis is an activated reaction, it is even more strongly disfavored compared to the other processes). In less polar solvents, such as dichloroethane, heterolytic cleavage is probably not competitive. Note that the COCl anion dissociates spontaneously to  $\text{CO} + \text{Cl}^-$ , which can recombine with the alkyl cation to yield alkyl chloride. Thus, the calculations do not lead us to expect major changes in the product composition from fragmentations of these alkoxychlorocarbenes on going from polar to nonpolar solvents.

(b) In the case of benzyloxychlorocarbene, the situation is different in various respects. First, due to the resonance energy of the incipient benzyl moiety, the transition states for all fragmentations fall significantly below that for cis-trans isomerization, so that the latter process is unlikely to be of importance in this case. Whereas the *trans*-carbene will undergo simple cleavage (homolytic in nonpolar, heterolytic in polar solvent), the *cis*-carbene will lose CO in a process whose exact mechanism was found to be difficult to assess, mainly because the predictions by different methods are at variance. According to spin-restricted B3LYP calculations, loss of CO requires only 7.5 kcal/mol of activation and leads via a  $\text{PhCH}_2^+\cdots\text{Cl}^-$  complex with a high degree of charge separation, which represents a transition state on the potential energy surface, to benzyl chloride. Unrestricted calculations show, however, that a diradicaloid state with a much smaller charge separation lies ca. 1 kcal/mol below the ion pair whose nature is therefore spurious.

In acetonitrile, the above ion pair turns into a minimum on the potential surface, which indicates that an ion pair of finite lifetime may also be involved in the decay of *cis*-benzyloxy-

chlorocarbene in sufficiently polar solvents. In the absence of suitable trapping agents this ion pair, which lies about 12 kcal/mol below individually solvated  $\text{PhCH}_2^+ + \text{Cl}^-$ , will, however, invariably decay to  $\text{PhCH}_2\text{Cl}$ . Thus, product analysis cannot yield any mechanistic information in this case.

Finally, we mention that preliminary experiments with cyclopropylmethoxychlorocarbene and cyclobutoxychlorocarbene indicate that the fragmentations and alkyl group rearrangements that afford mixtures of cyclopropylmethyl chloride, cyclobutyl chloride, and allylcarbinyl chloride in acetonitrile and dichloroethane<sup>28a,33</sup> persist in pentane. Given the unlikely intervention of ion pairs in the latter solvent, deep-seated concerted rearrangements must be coupled with the fragmentations of the carbenes. Further experimental and theoretical studies are planned.

## Experimental Section

**Solvents.** Acetonitrile, benzene, and pyridine (Fisher, Certified ACS) were refluxed over  $\text{CaH}_2$ , distilled, and stored over 5A molecular sieves. Dichloroethane, cyclohexane (Aldrich, Certified ACS), and pentane (Fisher, HPLC grade) were stored over 5A molecular sieves and then used directly.

**Diazirines.** The preparations of diazirines **6a**<sup>1,4</sup> and **6b**<sup>14</sup> have been described. Here we will detail the preparation of 3-*n*-octyloxy-3-chlorodiazirine (**6c**), and its precursor isouronium salt (**7c**), as illustrative of all cases.

*O-n-Octyloxyisouronium Trifluoromethanesulfonate* (**7c**,  $X = \text{OTf}$ ). This material was prepared by the general method of ref 13. 1-Octanol (20 mL, 127 mmol), cyanamide (1.07 g, 25 mmol), and trifluoromethanesulfonic acid (2.25 mL, 25 mmol) were stirred magnetically for 24 h at ambient temperature in a 100 mL round-bottom flask protected by a drying tube. Pentane (200 mL) was added, the mixture was refrigerated, and 6.0 g (73%) of **7c**, was harvested by filtration, recrystallized from  $\text{CH}_2\text{Cl}_2$  and dried in vacuo; mp 79–80 °C.  $^1\text{H}$  NMR ( $\delta$ ,  $\text{DMSO}-d_6$ ): 8.34–8.40 (br s, 4 H,  $2\text{NH}_2$ ), 4.22 (t,  $J = 6$  Hz, 2 H,  $\text{OCH}_2$ ), 1.66 (m, 2 H,  $\text{OCH}_2\text{CH}_2$ ), 1.23–1.27 (m, 10 H,  $(\text{CH}_2)_5$ ), 0.87 (crude t, 3 H,  $\text{CH}_3$ ).

Anal. Calcd. For  $\text{C}_{10}\text{H}_{21}\text{F}_3\text{N}_2\text{O}_4\text{S}$ : C, 37.23; H, 6.57; N, 8.70. Found: C, 37.01; H, 6.44; N, 8.60.

3-*n*-Octyloxy-3-chlorodiazirine (**6c**). The method of Graham was used.<sup>12</sup> Lithium chloride (4.2 g), DMSO (90 mL), isouronium salt **7c** (1.0 g, 3.1 mmol), and 40 mL of pentane were combined, stirred magnetically, and maintained at <20 °C (ice bath), while 150 mL of 12% commercial aqueous  $\text{NaOCl}$  ("pool chlorine"), saturated with  $\text{NaCl}$ , was added slowly over 30 min. The mixture was separated; the pentane phase was washed twice with ice water and then dried over  $\text{CaCl}_2$  at 0 °C for 2 h. The pentane solution of diazirine **6c** was passed through a short silica gel column. Pentane could then be removed by rotary evaporation and replaced by another solvent of choice (e.g., MeCN, benzene). About 30 mL of diazirine solution was thus prepared. UV:  $\lambda_{\text{max}}$  348, 366 nm (pentane); 362 nm (MeCN); 350, 370 nm (benzene).  $^1\text{H}$  NMR ( $\delta$ ,  $\text{C}_6\text{D}_6$ ): 3.48 (t,  $J = 6$  Hz, 2H,  $\text{OCH}_2$ ); 1.22–1.00 (m, 12 H,  $(\text{CH}_2)_6$ ); 0.84 (t,  $J = 7.5$  Hz, 3H,  $\text{CH}_3$ ).

**Photolysis of Diazirines.** Solutions of diazirines **6** (3 mL in solvent of choice,  $A \sim 1.0$  at  $\lambda_{\text{max}}$ ) were photolyzed in quartz cuvettes for 1 h at 25 °C with a focused 200 W Oriel UV lamp,  $\lambda > 320$  nm (uranium glass filter). UV spectroscopy indicated the absence of diazirine after photolysis. The photolysis products were analyzed by capillary GC and GC–MS using a 30 m  $\times$  0.32 mm  $\times$  0.25  $\mu\text{m}$  (film) HP-5 (5% PhMe siloxane) column at 30 °C (2 min), programmed to 260 °C at 30 deg/min. Products

were identified by GC and GC–MS comparisons to commercial or synthesized authentic samples. Product distributions are detailed in Tables 1, 3, and 4.

LFP experiments were performed with the apparatus described in ref 11.<sup>22</sup> Results are described above and in Table 5.

**Products from diazirine 6c.** 1-Octene (**10**) and 1-chlorooctane (**11**) were identified by comparisons to commercial samples. 2-chlorooctane (**12**) was prepared by the method of Hudson.<sup>34</sup> Thionyl chloride (13.7 mL, 189 mmol) was added dropwise with stirring to a mixture of 2-octanol (10 mL, 63 mmol) and pyridine (5.1 mL, 63 mmol). Overnight reflux afforded a brown liquid from which  $\text{SOCl}_2$  was stripped at the water pump. The residue was dissolved in 100 mL of ether, extracted with  $2 \times 100$  mL of brine, 100 mL of saturated aqueous  $\text{Na}_2\text{CO}_3$ , and again with 100 mL of brine. The ethereal phase was dried over  $\text{Na}_2\text{SO}_4$  and stripped, affording 7.0 g (47 mmol, 75%) of 2-chlorooctane.  $^1\text{H}$  NMR<sup>35</sup> ( $\delta$ ,  $\text{CDCl}_3$ ): 4.0 (m, 1 H,  $\text{CHCl}$ ); 1.67 (m, 2 H,  $\text{CH}_2\text{CHCl}$ ); 1.48 (d,  $J = 3$  Hz, 3 Hz, 3 H,  $\text{CH}_3\text{-CHCl}$ ); 1.26 (m, 8 H,  $\text{CH}_3(\text{CH}_2)_4$ ); 0.87 (m, 3 H,  $\text{CH}_3\text{CH}_2$ ). The sample also contained 1- and 2-octene.

1-Octyl formate (**13**) was prepared<sup>36</sup> from 3.5 mL (22 mmol) of 1-octanol, 8.0 mL (220 mmol) of formic acid, and 2.0 mL of boron trifluoride–dimethanol complex. The mixture was heated for 30 min at 85 °C, and then at 125 °C (reflux) for 1 h. Distillation at 45 °C then removed the  $\text{BF}_3$  complex. The residue was dissolved in 100 mL of ether, washed with  $2 \times 100$  mL of brine, saturated aqueous  $\text{Na}_2\text{CO}_3$  until no  $\text{CO}_2$  evolution was observed, and again with 100 mL of brine. The ether phase was dried over  $\text{Na}_2\text{SO}_4$ , and then stripped to give 2.6 g (16.4 mmol, 75%) of 1-octyl formate.  $^1\text{H}$  NMR<sup>37</sup> ( $\delta$ ,  $\text{CDCl}_3$ ): 7.91 (s, 1 H,  $\text{OCH}$ ); 4.00 (t,  $J = 6$  Hz, 2 H,  $\text{OCH}_2$ ); 1.49 (m, 2 H,  $\text{OCH}_2\text{CH}_2$ ); 1.12 (m, 10 H,  $(\text{CH}_2)_5$ ); 0.72 (t,  $J = 6$  Hz, 3 H,  $\text{CH}_3$ ).

**Matrix Isolation and Spectroscopy.** Diazirine **6a** was mixed with a 1000-fold excess of argon, and the mixture was deposited on a CsI crystal held at ca. 20 K inside an APD Cryogenics HC-2 closed-cycle cryostat. After about 5 mmol of Ar was deposited, the inlet valve was closed and the matrix was cooled to ca. 8 K. Irradiations at the wavelengths indicated in the text were effected with a 1 kW Hg–Xe lamp through the appropriate cutoff or interference filters. UV/vis spectra were recorded on a PE Lambda 900 instrument, and IR spectra were observed on a Bomem DA3 interferometer.

## Theoretical Methods

The geometries of all species were fully optimized by the B3LYP density functional method,<sup>38</sup> using the 6-31G\* basis set. All stationary points were characterized by second derivative calculations. In the case of  $\text{MeOCCl}$ , and at selected geometries of  $\text{PhCH}_2\text{OCCl}$ , stationary points were re-optimized in a dielectric continuum whose permittivity corresponds to that of acetonitrile, using the SCI-PCM method.<sup>39</sup> In the other cases, the same method was used in single-point calculations at the geometries optimized in vacuo to assess the influence of solvation.

Single-point calculations were also carried out by the coupled-cluster method, which accounts for the effect of single and double excitations and includes a perturbative estimate of triple excitations ( $\text{CCSD(T)}$ ), using Dunning's correlation-consistent polarized valence double- $\zeta$  (cc-pVDZ) and triple- $\zeta$  basis sets (cc-pVTZ, the latter only in the case of  $\text{MeOCCl}$ ).<sup>40,41</sup>

Atomic charges were calculated according to the ChelpG method.<sup>42</sup> All calculations were done with the implementation of the above methods in the Gaussian94<sup>43</sup> (solvation studies)



and Gaussian98<sup>44</sup> suites of programs. Cartesian coordinates and total energies (including thermal corrections) of all stationary points are available in ASCII form from the Supporting Information.

**Acknowledgment.** The authors at Rutgers and at Johns Hopkins are grateful to the National Science Foundation for financial support and to the center for Computational Neuroscience of Rutgers University (Newark) for computational support. J.P.T. acknowledges NSF Faculty Early Career Development and Camille Dreyfus Teacher-Scholar Awards. The work in Fribourg was supported by the Swiss National Science Foundation, project No. 2000-061560.00.

**Supporting Information Available:** Geometries for all structures optimized in this work and further information about partial atomic charges. This material is available free of charge via the Internet at <http://pubs.acs.org>.

## References and Notes

- (1) Moss, R. A.; Wilk, B. K.; Hadel, L. M. *Tetrahedron Lett.* **1987**, 28, 1969.
- (2) Moss, R. A.; Kim, H.-R. *Tetrahedron Lett.* **1990**, 31, 4715.
- (3) Moss, R. A. *Acc. Chem. Res.* **1999**, 32, 969.
- (4) Moss, R. A.; Ge, C.-S.; Maksimovic, L. *J. Am. Chem. Soc.* **1996**, 118, 9792.
- (5) Moss, R. A.; Johnson, L. A.; Yan, S.; Toscano, J. P.; Showalter, B. M. *J. Am. Chem. Soc.* **2000**, 122, 11256.
- (6) For ambiphilic carbenes such as **1**, methanolic trapping can be rather slow, with  $k \sim 10^4$ – $10^6$  s<sup>-1</sup>: Du, X.-M.; Fan, H.; Goodman, J. L.; Kesselmayr, M. A.; Krogh-Jespersen, K.; LaVilla, J. A.; Moss, R. A.; Shen, S.; Sheridan, R. S. *J. Am. Chem. Soc.* **1990**, 112, 1920.
- (7) Smith, N. P.; Stevens, I. D. R. *J. Chem. Soc., Perkin Trans. 2* **1979**, 1298.
- (8) Alkoxy- and aryloxychlorocarbenes exist in cis or trans forms, where partial double bond character restricts rotation about the O–C (carbene) bond: Kesselmayr, M. A.; Sheridan, R. S. *J. Am. Chem. Soc.* **1986**, 108, 99 and 844.
- (9) The question how to define an intimate ion pair arises here. We quote from a classic formulation by S. Winstein and G. C. Robinson of 1958: "some covalent character may be visualized for the cation–anion attraction in an intimate ion pair. ... Because of the character of intimate ion pairs, there is no sharp distinction between such an ion pair and a covalently bound intermediate in a so-called cyclic rearrangement. These are not qualitatively distinct, but form extremes in a graded series. Thus, there is no sharp distinction between formation of an intimate ion pair followed by internal return and a cyclic rearrangement, and marginal cases may be expected." Winstein, S.; Robinson, G. C. *J. Am. Chem. Soc.* **1958**, 80, 169.
- (10) B3LYP/6-31G\* with zero point energy correction: Yan, S.; Sauers, R. R.; Moss, R. A. *Org. Lett.* **1999**, 1, 1603.
- (11) Moss, R. A.; Johnson, L. A.; Merrer, D. C.; Lee, G. E., Jr. *J. Am. Chem. Soc.* **1999**, 121, 5940.
- (12) Graham, W. H. *J. Am. Chem. Soc.* **1965**, 87, 4396.
- (13) Moss, R. A.; Kaczmarczyk, G. M.; Johnson, L. A. *Synth. Commun.* **2000**, 30, 3233.
- (14) Diazirine **6b** (and isouronium salt **7b**) are described in: Johnson, L. A. Ph.D. Dissertation, Rutgers University, New Brunswick, NJ, 2001. For diazirine **6c**, see the Experimental Section.
- (15) Benzyl radical was observed spectroscopically upon LFP of **6a** in MeCN, DCE, or pentane solutions ( $\lambda$  303, 315 nm<sup>16</sup>). However, photolysis of **6a** in BrCCl<sub>3</sub> or cumene gave largely fragmentation product PhCH<sub>2</sub>Cl, rather than the radical products PhCH<sub>2</sub>Br (10%) or toluene (2%), suggesting a limited role for the benzyl radical.<sup>1</sup>
- (16) McAskill, N. A.; Sangster, D. F. *Aust. J. Chem.* **1977**, 30, 2107.
- (17) Baskir, E. G.; Maltsev, A. K.; Korolev, V. A.; Khabashesku, V. N.; Nefedov, O. M. *Izv. Akad. Nauk, Ser. Khim.* **1993**, 1499 (see entry for benzyl radical in <http://webbook.nist.gov>). In particular, the prominent peaks at 762 and 667 cm<sup>-1</sup> are indicative of the presence of the benzyl radical.
- (18) (a) Nicovitch, J. M.; Kreutter, P. H.; Wine, P. H. *J. Chem. Phys.* **1990**, 92, 3539. (b) From the calculated structure and the experimental vibrations of COCl (and the experimental entropies of CO and Cl),  $\Delta S$  for this process is about +23 cal K<sup>-1</sup> mol<sup>-1</sup>, so in the gas phase  $\Delta G(298\text{ K})$  is less than 1 kcal·mol<sup>-1</sup>. In solution, where the translational degrees of freedom of the two fragments are not fully realized,  $\Delta S$  is a bit smaller, but  $\Delta G$  is still so low that the lifetime of COCl is expected to be vanishingly small at room temperature.
- (19) Cf.: Moss, R. A.; Zheng, F.; Sauers, R. R.; Toscano, J. P. *J. Am. Chem. Soc.* **2001**, 123, 8109.
- (20) The dichloride product increased to 22% when carbene **4** was generated in benzene that contained 3.5 M added HCl. The dichloride was not formed in benzene that contained 4.0 M pyridine (which scavenges HCl<sup>4</sup>).
- (21) Jackson, J. E.; Soundararajan, N.; Platz, M. S.; Liu, M. T. H. *J. Am. Chem. Soc.* **1988**, 110, 5595.
- (22) For a description of our LFP system, see ref 11. The 1000 W Xe monitoring lamp described there has now been replaced with a Photophysics LS.1, 150 W pulsed Xe lamp light source.
- (23) In MeCN, ylide **21** absorbs at 460 nm.<sup>4</sup>
- (24) Ambiphilic carbenes (such as **1**) react "slowly" with pyridine;  $k_y = 9 \times 10^5$  for MeOCCl in MeCN: Ge, C.-S.; Jang, E. G.; Jefferson, E. A.; Liu, W.; Moss, R. A.; Wlostowska, J.; Xue, S. *Chem. Commun.* **1994**, 1479.
- (25) The average value of  $k_y = (2.9 \pm 0.2) \times 10^5$  M<sup>-1</sup> s<sup>-1</sup>.
- (26) (a) Iwata, K.; Hamaguchi, H. *Appl. Spectrosc.* **1990**, 44, 1431. (b) Yuzawa, T.; Kato, C.; George, M. W.; Hamaguchi, H. *Appl. Spectrosc.* **1994**, 48, 684. (c) Toscano, J. P. *Adv. Photochem.* **2001**, 26, 41.
- (27) At [Cl<sup>-</sup>] = 0, the Y-intercept of Figure 4 should equal  $k_{\text{obs}}$  for the formation of ylide at 5.77 M pyridine. Agreement is observed; the intercept is  $2.5 \times 10^6$  s<sup>-1</sup>, whereas the experimental  $k_{\text{obs}} = 2.7 \times 10^6$  s<sup>-1</sup>.
- (28) (a) Moss, R. A.; Zheng, F.; Johnson, L. A.; Sauers, R. R. *J. Phys. Org. Chem.* **2001**, 14, 400. (b) Moss, R. A.; Zheng, F.; Fede, J.-M.; Ma, Y.; Sauers, R. R.; Toscano, J. P.; Showalter, B. M. *J. Am. Chem. Soc.* **2002**, 124, 5258.
- (29) The different quantum chemical methods employed in this work differ strongly in their prediction of  $D_0$  of the COCl radical (B3LYP/6-31G\*, +11.45; CCSD(T)/cc-pVDZ, -0.45; CCSD(T)/cc-pVTZ, +4.1 kcal/mol), so that we prefer to use experimental data here.
- (30) COCl<sup>-</sup> is not bound and undergoes activationless cleavage to CO + Cl<sup>-</sup> even in the gas phase.
- (31) Note that according to IRC calculations, fragmentation occurs from a slightly different conformer of the *cis*-carbene which lies a fraction of a kcal/mol above the lowest energy structure (cf., Figure 10).
- (32) Reoptimization of the complex with UB3LYP (Guess=mix., always) led to a slightly different geometry, which did, however, still represent a saddle point on the potential surface.
- (33) Moss, R. A.; Ho, G. J.; Wilk, B. K. *Tetrahedron Lett.* **1989**, 30, 2473.
- (34) Hudson, H. R.; Spinoza, G. R. *J. Chem. Soc., Perkin Trans. I* **1976**, 104.
- (35) Troyanskii, E. I.; Svitani'ko, I. V.; Ogibin, Y. N.; Nikishin, G. I. *Bull. Akad. Sci. USSR, Div. Chem. Sci.* **1983**, 10, 2090.
- (36) Dymicky, M. *Org. Prep. Proced. Int.* **1982**, 14, 177.
- (37) Safiev, O. G.; Kruglov, D. E.; Popov, Y. N.; Zlotnik, S. S.; Rakhmankulov, D. L. *J. Org. Chem. USSR* **1984**, 20, 997.
- (38) (a) Becke, A. D. *J. Chem. Phys.* **1993**, 98, 5648. (b) Lee, C.; Yang, W.; Parr, R. G. *Phys. Rev. B* **1998**, 37, 785.
- (39) Foresman, J. M.; Keith, T. A.; Wiberg, K. B. *J. Phys. Chem.* **1996**, 100, 16098. Self-consistent reaction field methods model solvation effects in terms of a reaction field with a uniform dielectric constant. The SCI-PCM routine takes into account the importance of coupling the isodensity surface and the electron density, and, as such, includes the effect of solvation in the SCF computations.
- (40) (a) Woon, D. E.; Dunning, T. H. Jr. *J. Chem. Phys.* **1993**, 98, 1358. (b) Dunning, T. H., Jr. *J. Chem. Phys.* **1989**, 90, 1007.
- (41) (a) Scuseria, G. E.; Schaefer, H. F., III. *J. Chem. Phys.* **1989**, 90, 3700. (b) Pople, J. A.; Head-Gordon, M.; Raghavachari, K. *J. Chem. Phys.* **1987**, 87, 5968.
- (42) Breneman, C. M.; Wiberg, K. B. *J. Comput. Chem.* **1990**, 11, 361.
- (43) Frisch, M. J.; Trucks, G. W.; Schlegel, H. B.; Gill, P. M. W.; Johnson, B. G.; Robb, M. A.; Cheeseman, J. R.; Keith, T.; Petersson, G. A.; Montgomery, J. A.; Raghavachari, K.; Al-Laham, M. A.; Zakrzewski, V. G.; Ortiz, J. V.; Foresman, J. B.; Cioslowski, J.; Stefanov, B. B.; Nanayakkara, A.; Challacombe, M.; Peng, C. Y.; Ayala, P. Y.; Chen, W.; Wong, M. W.; Andres, J. L.; Replogle, E. S.; Gomperts, R.; Martin, R. L.; Fox, D. J.; Binkley, J. S.; Defrees, D. J.; Baker, J.; Stewart, J. P.; Head-Gordon, M.; Gonzalez, C.; Pople, J. A. *Gaussian 94*, revision E.2; Gaussian, Inc.: Pittsburgh, PA, 1995.
- (44) Frisch, M. J.; Trucks, G. W.; Schlegel, H. B.; Scuseria, G. E.; Robb, M. A.; Cheeseman, J. R.; Zakrzewski, V. G.; Montgomery, J. A., Jr.; Stratmann, R. E.; Burant, J. C.; Dapprich, S.; Millam, J. M.; Daniels, A. D.; Kudin, K. N.; Strain, M. C.; Farkas, O.; Tomasi, J.; Barone, V.; Cossi, M.; Cammi, R.; Mennucci, B.; Pomelli, C.; Adamo, C.; Clifford, S.; Ochterski, J.; Petersson, G. A.; Ayala, P. Y.; Cui, Q.; Morokuma, K.; Malick, D. K.; Rabuck, A. D.; Raghavachari, K.; Foresman, J. B.; Cioslowski, J.; Ortiz, J. V.; Baboul, A. G.; Stefanov, B. B.; Liu, G.; Liashenko, A.; Piskorz, P.; Komaromi, I.; Gomperts, R.; Martin, R. L.; Fox, D. J.; Keith, T.; Al-Laham, M. A.; Peng, C. Y.; Nanayakkara, A.; Gonzalez, C.; Challacombe, M.; Gill, P. M. W.; Johnson, B.; Chen, W.; Wong, M. W.; Andres, J. L.; Gonzalez, C.; Head-Gordon, M.; Replogle, E. S.; Pople, J. A. *Gaussian98*, revision A.7; Gaussian, Inc.: Pittsburgh, PA, 1998.